Correlated Inhibitory and Excitatory Inputs to the Coincidence Detector: Analytical Solution

Shawn Mikula and Ernst Niebur

***Abstract*—We present a solution for the steady-state output rate of an ideal coincidence detector receiving an arbitrary number of excitatory and inhibitory input spike trains. All excitatory spike trains have identical binomial count distributions (which includes Poisson statistics as a special case) and arbitrary pairwise cross correlations between them. The same applies to the inhibitory inputs, and the rates and correlation functions of excitatory and inhibitory populations may be the same or different from each other. Thus, for each population independently, the correlation may range from complete independence to perfect correlation (identical processes). We find that inhibition, if made sufficiently strong, will result in an inverted U-shaped curve for the output rate of a coincidence detector as a function of input rates for the case of identical inhibitory and excitory input rates. This leads to the prediction that higher presynaptic (input) rates may lead to lower postsynaptic (output) rates where the output rate may fall faster than the inverse of the input rate, and shows some qualitative similarities to the case of purely excitatory inputs with synaptic depression. In general, we find that including inhibition invariably and significantly increases the behavioral repertoire of the coincidence detector over the case of pure excitatory input.**

***Index Terms*—Coincidence detector, inhibition, neural code, synchrony.**

I. Introduction

DECIPHERING the neuronal code is one of the central problems in neuroscience. The earliest studies [2] found regular firing (with adaptation) of primary afferent neurons in response to constant stimulation and their authors suggested a frequency (rate) code of sensory input. In the central nervous system (CNS), random-walk models, based on Poisson statistics, proved useful for explaining at least part of the statistics of spike activity [11]. However, although these methods were considerably refined in future work [22], [32], more complex firing patterns that were not consistent with Poisson statistics were identified in the CNS early on [19], [33]. Subsequent work added more doubt at the idea of the brain as a network of independently firing stochastic elements using a rate code for communication and computation. For instance, Softky and Koch [28], [29] pointed out that the large convergence of CNS neurons in combination with independently firing presynaptic neurons obeying Poisson statistics necessarily leads to regular (periodic) postsynaptic firing which is not observed. Different solutions have been proposed to this conundrum [9], [23], [25], [27] and a significant part of the ensuing discussion has been on the effects of correlated neuronal activity. This development is consistent with the growing understanding that complex time structures and correlations within neuronal populations play important roles for determining receptive field properties and for neural coding in general [4], [6], [10], [17], [18], [21], [24], [26], [30]. Despite the fact that inhibitory neurons comprise a significant portion of the neuronal population (about 20%–30% within primate cortex [12]), there is currently no strong consensus on the exact roles of inhibition in neuronal coding. Particularly desirable would be insight gained from analytical solutions. In this paper, we determine analytically the effects of rate- and synchrony-modulated inhibition on neuronal output responses and on neural coding in one of the simplest neural models, the coincidence detector.

Using combinatorial methods, we have previously found the analytical solution for the output rate of an ideal coincidence detector that receives an arbitrary number of input spike trains with identical binomial count distributions (which includes Poisson statistics as a special case) and identical pairwise cross correlations either for fixed [15] or depressing [16] synapses. That is, we analytically determined the output response of a coincidence detector as a function of input rate and input cross correlation.

The solution in the previous studies only allowed excitatory inputs. In this paper, we overcome this limitation by extending our previous results to include the practically important case of inhibitory inputs. The solution developed here is for arbitrary numbers of excitatory and inhibitory input spike trains, with arbitrary rates and cross correlations within and between the populations of excitatory and inhibitory spike trains.

II. Methods

A. Model Neurons: Coincidence Detectors

The model neurons used in this study are coincidence detectors, that is, computational units that fire at time t if an internal state variable (a model of the transmembrane voltage at the location where action potentials are generated) equals or exceeds a threshold θ. The value of this variable is determined by the balance of excitatory and inhibitory synaptic inputs arriving within the window $[t-T,\ t]$. All our results will be generally valid for any time interval T; a physiologically plausible value for T is the integration period of fast synapses, that is, on the order of 5 ms.

B. Binomial Spike Trains with Specific Cross Correlation

In our previous paper [15], we introduced a systematic method for the generation of an arbitrary number of spike trains

Manuscript received May 27, 2003; revised January 7, 2004. This work was supported in part by the National Science Foundation under a CAREER Grant and in part by the National Institutes of Health-National Institute of Neurological Disorders and Diseases (NINDS) under Grant NS43188-01A1.

The authors are with The Krieger Mind/Brain Institute and the Department of Neuroscience, The Johns Hopkins University, Baltimore, MD 21218 USA.

Digital Object Identifier 10.1109/TNN.2004.832708

with specified pair-wise mean cross correlations and firing rates.[1] Spikes are distributed according to binomial counting statistics in each spike train. Mean firing rates and cross correlations are the same for all spike trains (or all pairs of spike trains, respectively), but they can be chosen independently of each other. The algorithm that we describe here is both suitable for the analytical computations in this paper as for the implementation of such spike trains in numerical simulations. We emphasize that, although we will use this particular algorithm to illustrate the derivation of the output rate of the coincidence detector in this paper, our results are of general validity since the properties of the spike trains are entirely specified by their correlation coefficient and the statistics of the individual spike trains. However, no higher order effects (correlations of order 3 and higher; see, e.g., [5]) are included.

Let m be the number of input spike trains, each having n time bins. All bins are of equal length δt, chosen sufficiently small so that each contains a maximum of one spike, that is, each bin is guaranteed to contain either one or zero spikes. The coincidence detector makes the decision whether to fire or not within one time bin, therefore, $T = \delta t$. Assuming a firing rate of

$$f = \frac{p}{\delta t} \tag{1}$$

the probability that a spike is found in any given time bin is p; no spike is found with probability $(1 - p)$. Bins in any given spike train are independent of each other which implies that the following analysis can be limited to a single time bin. Note that the physiologically important Poisson statistics are the special case of low rates (or correspondingly, low-spike probabilities).

A set of m spike trains (with $m \geq 2$) with a Pearson correlation coefficient q (with $0 \leq q \leq 1$) between any two of them is constructed as follows. We start by generating $m + 1$ *independent* spike trains with mean firing rates f and designate spike train number $m+1$ as the "reference spike train." In order to introduce the correlation coefficient q between spike trains $= 1, 2, \ldots, m$, we switch, with a probability $\sqrt{q}$, the state (one or zero spikes) of a time bin in each of these spike trains to that found in the reference spike train. This yields a mean correlation coefficient of q between any two of the spike trains $1, \ldots, m$ while maintaining the mean firing rate as $p/\delta t$. We showed [16] that q is, indeed, the usual Pearson correlation coefficient.

For the purposes of the present study, we generate two sets of synapses. The first set of m_e excitatory synapses[2] receives input from stochastic spike trains with a mean rate of $p_e/\delta t$ and a Pearson correlation coefficient q_e between any two spike trains. The second set, comprising m_i inhibitory synapses receives input from spike trains with a mean rate $p_i/\delta t$ and a correlation coefficient q_i. We allow for different weights of excitatory and inhibitory synapses; without loss of generality we set the former to unity and the latter to $r > 0$. Fig. 1 illustrates the collection of synaptic inputs and the decision process in the coincidence detector.

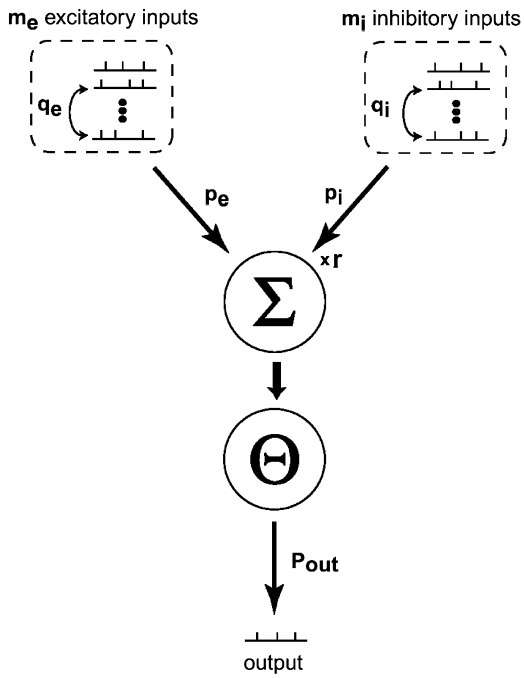

Fig. 1. Overview of the model and notation. The coincidence detector receives m_e excitatory inputs with mean spike probability p_e per time bin and mean cross correlation q_e between spike trains. In addition, it receives m_i inhibitory inputs with mean spike probability p_i per time bin and mean cross correlation q_i. Excitatory synapses have unit weight and inhibitory synapses have a relative weight r. Weighted inputs are summed (Σ), with inhibitory synapses counted negatively, and a spike is generated if the weighted sum exceeds the threshold (θ). The output firing probability in a given time bin is P_{out}.

III. Results

A. Coincidence Detection for Uncorrelated Inputs

It is useful to first consider the special case of independent input spike trains, i.e., $q_e = q_i = 0$. Thus, in the following, we will derive the equation for $P_{\text{out}}(p_e, p_i, m_e, m_i, r, \theta, q_e = 0, q_i = 0)$, the output spiking probability (P_{out}) of a coincidence detector as a function of threshold (θ), number of excitatory inputs (m_e) and their input spike probability (p_e), the number of inhibitory inputs (m_i) and their input spike probability (p_i), and the ratio of inhibitory input spike strength to excitatory input spike strength (r). Let $\bar{j}$ be the random variable denoting the number of excitatory input spikes and let $\bar{J}$ be the random variable denoting the number of inhibitory input spikes. Then a suprathreshold event occurs if and only if $j - J \cdot r \geq \theta$, where j and J are realizations of $\bar{j}$ and $\bar{J}$, respectively. Let the probability of this be $P(\bar{j} - \bar{J} \cdot r \geq \theta)$ (which is the same as P_{out} above). We can represent $P(\bar{j} - \bar{J} \cdot r \geq \theta)$ as the following joint probability:

$$P(\bar{j} - \bar{J} \cdot r \geq \theta) = P(\bar{j} - \bar{J} \cdot r \geq \theta \mid \bar{j} \geq \theta) \cdot P(\bar{j} \geq \theta) \tag{2}$$

where $P(\bar{j} - \bar{J} \cdot r \geq \theta \mid \bar{j} \geq \theta)$ and $P(\bar{j} \geq \theta)$ are conditional and marginal probabilities, respectively. It is a trivial matter to

[1]The method used here is not the only possible way to introduce correlations between spike trains. For instance, one could add spikes generated by a common Poisson process to each individual spike train [31], or start from a common spike train and generate two different spike trains by removing spikes independently [14]. Feng and Brown [9] study pairwise correlations with a more general approach than ours, allowing structures like "block type" (locally constant) and Gaussian-type correlations, but their method is not constructive. The method presented here has the advantage of being straightforward and efficient, and of generating spike trains with controlled rates and correlation coefficients, both of which being determined in a direct way.

[2]We will always assume $m_e \geq \theta$ since otherwise we only get the trivial solution with no output spikes.

rearrange $\bar{j} - \bar{J} \cdot r \geq \theta$ to yield the following expression:

$$P(\bar{j} - \bar{J} \cdot r \geq \theta) = P\left(\bar{J} \leq \frac{\bar{j} - \theta}{r} \mid \bar{j} \geq \theta\right) \cdot P(\bar{j} \geq \theta). \quad (3)$$

The second term on the right-hand side, the marginal probability, $P(\bar{j} \geq \theta)$, is the sum over probabilities for j excitatory input spikes, such that $j \geq \theta$. We showed previously [16] that $P(\bar{j} \geq \theta)$ is given by the following binomial distribution:

$$P(\bar{j} \geq \theta) = \sum_{j=\theta}^{m_e} \binom{m_e}{j} (1 - p_e)^{m_e - j} \quad (4)$$

which is the sum over all probabilities for having j excitatory input spikes such that $j \geq \theta$.[3]

The first term on the right-hand side of (3), the conditional probability, $P(\bar{J} \leq (\bar{j} - \theta)/r \mid \bar{j} \geq \theta)$, is the sum over probabilities for having J inhibitory input spikes given that the number of excitatory spikes equals or exceeds threshold. This conditional probability becomes the simple probability

$$P\left(\bar{J} \leq \frac{\bar{j} - \theta}{r} \mid \bar{j} \geq \theta\right) = P\left(\bar{J} \leq \frac{\bar{j} - \theta}{r}\right) \quad (5)$$

if we can assure $j \geq \theta$. The right-hand side of (5) can be computed in analogy to (4) and found to be [15]

$$P\left(\bar{J} \leq \frac{\bar{j} - \theta}{r}\right) = \sum_{J=0}^{L((j-\theta)/r)} \binom{m_i}{J} p_i^J (1 - p_i)^{m_i - J} \quad (6)$$

where $L(x)$ is the *floor* function (also denoted by $\lfloor x \rfloor$ in the literature) that rounds its (positive) argument down to the nearest integer.

Substituting (4) and (6) into (3), we arrive at the expression for $P(\bar{j} - \bar{J} \cdot r \geq \theta)$

$$P\left(\bar{j} - \bar{J} \cdot r \geq \theta\right) = \sum_{j=\theta}^{m_e} \binom{m_e}{j} p_e^j (1 - p_e)^{m_e - j} \cdot \sum_{J=0}^{L((j-\theta)/r)} \binom{m_i}{J} p_i^J (1 - p_i)^{m_i - J}. \quad (7)$$

It is seen that the condition $j \geq \theta$ needed to derive 5 is fulfilled by the range of the index in the first summation in (7).

Finally, noting that $P(\bar{j} - J \cdot r \geq \theta) = P_{\text{out}}(p_e, p_i, m_e, m_i, r, \theta, q_e = 0, q_i = 0)$, and rearranging terms slightly from (7), we arrive at the following:

$$P_{\text{out}}(p_e, p_i, m_e, m_i, r, \theta, q_e = 0, q_i = 0) = \sum_{j=\theta}^{m_e} \sum_{J=0}^{L((j-\theta)/r)} \binom{m_e}{j} p_e^j (1 - p_e)^{m_e - j} \binom{m_i}{J} \cdot p_i^J (1 - p_i)^{m_i - J} \quad (8)$$

which is the probability for a coincidence detector to produce an output spike given m_e uncorrelated excitatory input spike trains with mean spike probability p_e and m_i inhibitory input spike trains with a spike strength of r times the excitatory input spike strength, and with mean spike probability p_i.

[3]Technically, one should use a running index different from j in the sum on the right-hand side, but this would increase notational complexity and the present notation should not lead to ambiguities. The same applies to the use of J in (6) and later.

B. Positive Correlation

In the following, we will generalize (8) to the case when excitatory inputs are correlated with Pearson correlation q_e and inhibitory inputs are correlated with Pearson correlation q_i. The derivation is exactly analogous to the one employed in Section III-A. Indeed, (3) is valid in this section as well and the key difference resides in the meanings of the terms in this equation. For instance, the marginal probability $P(j \geq \theta)$ retains the same interpretation as before but it becomes slightly more complicated to account for the effects of input cross correlation.

If only excitatory inputs with correlation q_e are present, we showed [16] that $P(j \geq \theta)$ is given by

$$p(\bar{j} \geq \theta) = \sum_{j=\theta}^{m_e} \Bigg\{ \sum_{k=j}^{m_e} \binom{m_e}{k} p_e^k (1 - p_e)^{m_e - k} \binom{k}{j} \cdot \sqrt{q_e}^{k-j} (1 - \sqrt{q_e})^j (1 - p_e) + \sum_{k=0}^{j} \binom{m_e}{k} p_e^k (1 - p_e)^{m_e - k} \binom{m_e - k}{j - k} \cdot \sqrt{q_e}^{j-k} (1 - \sqrt{q_e})^{m_e - j} p_e \Bigg\} \quad (9)$$

which is a sum over all the probabilities for having j excitatory input spikes such that $j \geq \theta$. We refer to [15] for the detailed derivation of this result and only give a brief intuitive overview. Equation (9) is obtained from the simpler result for uncorrelated spike trains, (4), by observing that the correlation between m_e spike trains can be formally characterized by their interaction with the "reference spike train," introduced in Section II-B. The solution in (4) then has to be generalized to take into account the effect of the state changes in each spike train by the procedure described in Section II-B, that is, changing the state in each spike train to that in the reference spike train with probability q_e. There are two cases in which this will modify the output of the coincidence detector: either the state of a sufficient number of the m_e spike trains will be changed from "no-spike" to "spike," or the opposite. The first and second terms in the braces sum the probabilities for the first and the second of these possibilities, respectively. It goes without saying that (4) is the special case $q_e = 0$ of (9).

The derivation of the conditional probability, $P(\bar{j} - \bar{J} \cdot r \geq \theta \mid \bar{j} \geq \theta)$ in (3) is exactly analogous to the one employed in Section III-A leading to the derivation of (6), except that we now employ (9) instead of (4) to obtain the following:

$$P(\bar{j} - \bar{J} \cdot r \geq \theta \mid \bar{j} \geq \theta) = \sum_{J=0}^{L((j-\theta)/r)} \Bigg\{ \sum_{K=J}^{m_i} \binom{m_i}{K} p_i^K (1 - p_i)^{m_i - K} \binom{K}{J} \cdot \sqrt{q_i}^{K-J} (1 - \sqrt{q_i})^J (1 - p_i) + \sum_{K=0}^{J} \binom{m_i}{K} \cdot p_i^K (1 - p_i)^{m_i - K} \binom{m_i - K}{J - K} \cdot \sqrt{q_i}^{J-K} (1 - \sqrt{q_i})^{m_i - J} p_i \Bigg\}. \quad (10)$$

Now, substituting (9) and (10) into (3), noting that $P(\bar{j} - \bar{J} \cdot r \geq \theta) = P_{\text{out}}(p_e, p_i, q_e, q_i, m_e, m_i, r, \theta)$, and rearranging terms slightly, we arrive at (11), shown at the bottom of the page.

Equation (11) is our main result. It is a closed expression for the output rate of a coincidence detector receiving an arbitrary number of inhibitory and excitatory inputs with identical binomial statistics and modulated both with respect to mean rate and cross correlation.

IV. Example

We illustrate the key properties of (11) with an example calculation using the following parameters: $m_e = 45$, $m_i = 15$, $r = 8$, and $\theta = 13$. We note that the percentage of inhibitory inputs in our example (25%) is consistent with the observed percentage of inhibitory neurons in primate cerebral cortex, which ranges from 20% to 30% [12]. The value of r, denoting the ratio of inhibitory input strength to excitatory input strength, is somewhat on the high end but compatible with empirical and analytical estimates of about five [8]. Though many computational studies have assumed "balanced inhibition" [1], [7], [20], [26], which would result in $r = 3$ in our model (i.e., $r \times m_i = m_e$), we choose not to make this assumption, for two reasons. The first is that it is far from proven that balanced inhibition is in the physiological parameter range and, in fact, some evidence exists that this is not the case, at least not in any exact sense [10], [13]. The second reason is that, for this example, using a relatively high value of $r = 8$ serves to better accentuate the effects attributed to the inhibitory inputs.

Differentially rate- and synchrony-modulated inhibitory inputs greatly add to the structural complexity of a coincidence detector. While a coincidence detector with exclusively excitatory inputs is completely characterized by four independent parameters (m_e, p_e, q_e, θ), this number doubles in the case of the current system, (11) (additionally m_i, p_i, q_i and r). The increase in structural complexity is reflected in a concomitant increase in behavioral complexity. Even if we reduce the number of degrees of freedom to six by fixing the relationships between relative numbers and strengths of excitatory and inhibitory synapses using the physiological and anatomical constraints described in the previous paragraph, the model shows a much larger range of behaviors than was observed with purely excitatory input [15], [16].

Figs. 2 and 3 illustrate the increase in the diversity of response surfaces. For instance, depending on the cross correlation of the inhibitory inputs, the output rate can either increase [Fig. 3(c)] or decrease [Fig. 3(d)] as a function of excitatory input cross correlation. As is evident in both figures as well as in Fig. 3(b), the output rate is a nonmotonic function of input rate, increasing with the input spike probability when the latter is low and decreasing when it is high. This seemingly counterintuitive behavior (decreased output rate for increased input rate) is not present with purely excitatory input and fixed synapses [Fig. 3(a)] but we note that it is also observed in the coincidence detector with depressing synapses [16]. As another example of behavioral features added by the inclusion of inhibitory input, we note that output rate often increases as inhibitory input synchrony is increased [(Fig. 2(b)]. This is related to the observation that output rate often decreases as excitatory input synchrony is increased [also seen in Fig. 2(d)]. Both effects are due to inefficient allocation (or "wasting") of input spikes, first observed in numerical studies (of purely excitatory neurons) by Bernander *et. al* [3].

Some special cases can be easily observed in these figures. For instance, the transformation of the input probability into the output probability is greatly simplified in the case of strong, identical excitatory and inhibitory correlation, $q_e = q_i = 1$ [rightmost bounding curve in Fig. 3(b)]. Since all excitatory inputs are now synchronous, and likewise all inhibitory inputs are synchronous, the resulting output probability is related to the input by the logistic function,

$$P_{\text{out}} = p_e(1 - p_i) = p_e(1 - p_e) \tag{12}$$

where the second equality results from $p_e = p_i$, assumed in all calculations illustrated in Fig. 3. The validity of the first equality can be seen since an output spike can only be generated if the excitatory input population spikes which occurs with probability p_e. Since $m_i \times r > m_e$, a volley of the inhibitory population "vetoes" any output spike; such a volley occurs with probability p_i and its absence, therefore, with probability $(1 - p_i)$. By assumption the excitatory and inhibitory populations are independent, and we obtain the first equality in (12). This behavior is visually confirmed by inspection of Fig. 3(b).

The qualitative behavior (though not the exact values) on the line $q_e = 1$ is similar in the case of fixed moderate correlation

$$\begin{aligned}
&P_{\text{out}}(p_e, p_i, q_e, q_i, m_e, m_i, r, \theta) \\
&\quad = \sum_{j=\theta}^{m_e} \sum_{J=0}^{L((j-\theta)/r)} \left\{ \sum_{k=j}^{m_e} \binom{m_e}{k} p_e^k (1-p_e)^{m_e-k} \binom{k}{j} \sqrt{q_e}^{k-j} (1-\sqrt{q_e})^j (1-p_e) \right. \\
&\qquad \left. + \sum_{k=0}^{j} \binom{m_e}{k} p_e^k (1-p_e)^{m_e-k} \binom{m_e-k}{j-k} \sqrt{q_e}^{j-k} (1-\sqrt{q_e})^{m_e-j} p_e \right\} \\
&\qquad \times \left\{ \sum_{K=J}^{m_i} \binom{m_i}{K} p_i^K (1-p_i)^{m_i-K} \binom{K}{J} \sqrt{q_i}^{K-J} (1-\sqrt{q_i})^J (1-p_i) + \right. \\
&\qquad \left. + \sum_{K=0}^{J} \binom{m_i}{K} p_i^K (1-p_i)^{m_i-K} \binom{m_i-K}{J-K} \sqrt{q_i}^{J-K} (1-\sqrt{q_i})^{m_i-J} p_i \right\}.
\end{aligned} \tag{11}$$

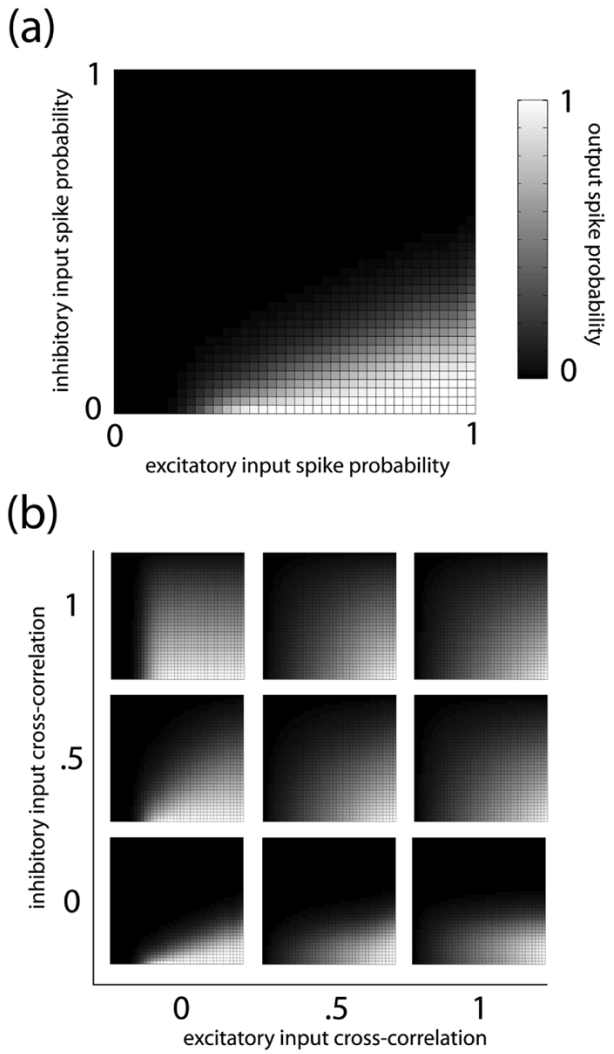

Fig. 2. Analytical solution of the coincidence detector as function of input rates of excitatory (abscissa) and inhibitory (ordinate) input rate. The probability of an output spike is shown in gray shading with the key for the gray scale used in all subfigures being shown at right in part a. (a) Parameters: $m_e = 45$, $m_i = 15$, $\theta = 13$, $r = 8$, $q_e = 0$, $q_i = 0$. (b) Same parameters as (a) but now for three different values (0, 0.5, and 1) for $q_e = q_i$, varying along the main axes. Although the general tendency is as expected, with spiking probability low in the top left corner and high in the bottom right corner, the detailed behavior shows deviations from this scheme. Some of them are explored in Fig. 3.

between inhibitory inputs, $q_i = 0.5$ as shown in Fig. 3(d). The behavior in these two cases is very different, however, for small q_e. When all inputs are independent [$q_e = q_i = 0$, in Fig. 3(b)], P_{out} falls essentially to zero. This is due to the fact that there are always at least some inhibitory synapses active and because of their larger weights they essentially always "veto" any output activity (again, since $r \times m_i > m_e$). In contradistinction, for moderately correlated inhibitory inputs $q_i = 0.5$, the probability for an output spike *increases*[4] when the correlation of excitatory inputs *decreases* because the "wasting" of excitatory synaptic inputs is less pronounced [$q_e = 0$ line in Fig. 3(d)].

[4]At least for intermediate input rates; other factors play a role for very high and very low rates.

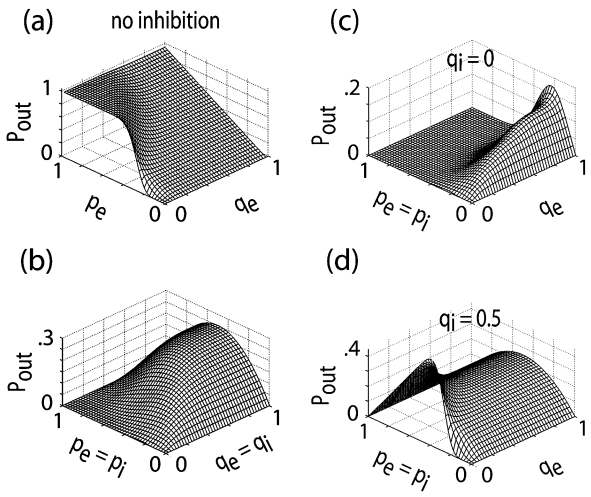

Fig. 3. Influence of inhibition on the coincidence detector. Contour plots show the output spike probability (z-axis) as function of mean input frequencies, assumed identical for excitatory and inhibitory inputs $p_e = p_i$. Other parameters common to all plots are $m_e = 45, \theta = 13$, and $r = 8$. The four plots differ by the type of inhibition. (a) No inhibition ($m_i = 0$). Sigmoidal increase with input frequency for $q_e = 0$ changes smoothly into linear behavior (one input volley generating one output spike) for $q_e = 1$. (b) Excitatory correlation equal to inhibitory correlation, $q_i = q_e$. (c) Uncorrelated inhibitory input, $q_i = 0$. (d) Moderately correlated inhibitory input, $q_i = 0.5$.

V. Discussion

In this paper, we determine analytically the effects of rate- and synchrony-modulated inhibition on neuronal output responses. Most work so far has focused on excitatory synaptic action, but given the prominence of inhibitory populations in neocortex, it is highly desirable to gain deeper insight into the function of neuronal inhibition. This paper extends our previous analytical results [15], [16] for a coincidence detector to account for inhibitory inputs. The solution is for the steady-state output of an ideal coincidence detector receiving an arbitrary number of input spike trains with identical binomial count distributions (which includes Poisson statistics as a special case) and identical arbitrary pairwise cross correlations, from zero correlation (independent processes) to perfect correlation (identical processes). The main result is (11). Figs. 2 and 3 are examples of cuts through the eight-dimensional parameter space.

Our derivation is based on a simple model and it is important to make explicit the key assumptions of our model given by: 1) the bins in any given input spike train are independent; 2) the excitatory and inhibitory subpopulations are not correlated with each other; and 3) the coincidence detector "neuron" integrates over a very short time window. The first condition, which is equivalent to saying that the input spike train statistics are Poisson, means that additional effects may exist that depend on the structure of the individual spike trains (e.g., oscillations). The second condition has similar consequences for structures in the correlation between excitatory and inhibitory populations. The third condition makes the model memoryless, which serves to differentiate it from integrator models with long time constants. We feel that these simplifications are justified in the interest of obtaining an analytical solution.

We find that inhibition, if made sufficiently strong, will result in an inverted U-shaped curve for the output rate of a co-

incidence detector as a function of input rates for the case of identical inhibitory and excitory input rates. This leads to the counterintuitive prediction that higher presynaptic (input) rates may lead to lower postsynaptic (output) rates where the output rate may fall faster than the inverse of the input rate, and shows some qualitative similarities to the case of purely excitatory inputs with synaptic depression [16]. In general, the inclusion of inhibitory inputs increases the variability of output responses as a function of input spike train parameters, which includes the degree of synchrony and rate within inhibitory and excitatory inputs.

In summary, we believe our derivation will prove useful both as a theoretical example highlighting the utility of combinatorial methods for deriving exact solutions in terms of relevant parameters and variables, and in explaining the relative contributions of excitation *versus* inhibition, and rate *versus* synchrony in neural coding.

REFERENCES

[1] M. Abeles, *Corticonics: Neural Circuits of the Cerebral Cortex*. Cambridge, U.K.: Cambridge Univ. Press, 1991.

[2] E. D. Adrian and Y. Zotterman, "The impulses produced by sensory nerve endings. Part 2. The response of a single end organ," *J. Physiol.*, vol. 61, pp. 151–171, 1926.

[3] O. Bernander, C. Koch, and M. Usher, "The effect of synchronized inputs at the single neuron level," *Neural Computat.*, vol. 6, no. 4, pp. 622–641, 1994.

[4] A. Bibbig, R. Traub, and M. Whittington, "Long-range synchronization of gamma and beta oscillations and the plasticity of excitatory and inhibitory synapses: A network model," *J. Neurophysiol.*, vol. 88, pp. 1634–54, 2002.

[5] S. M. Bohte, H. Spekreijse, and P. R. Roelfsema, "The effects of pairwise and higher-order correlations on the firing rate of a postsynaptic neuron," *Neural Computat.*, vol. 12, pp. 153–179, 2000.

[6] C. Borgers and N. Kopell, "Synchronization in networks of excitatory and inhibitory neurons with sparse, random connectivity," *Neural Computat.*, vol. 15, no. 3, pp. 509–538, 2003.

[7] P. C. Bush and T. J. Sejnowski, "Effects of inhibition and dendritic saturation in simulated neocortical pyramidal cells," *J. Neurophysiol.*, vol. 71, no. 6, pp. 2183–93, 1994.

[8] A. Destexhe, M. Rudolph, and D. Pare, "The high-conductance state of neocortical neurons in vivo," *Nature Neurosci. Rev.*, vol. 4, pp. 739–751, 2003.

[9] J. Feng and D. Brown, "Impact of correlated inputs on the output of the integrate- and-fire model," *Neural Computat.*, vol. 12, no. 3, pp. 671–92, 2000.

[10] J. Feng, G. Li, D. Brown, and H. Buxton, "Balance between four types of synaptic input for the integrate-and-fire model," *J. Theory Biol.*, vol. 7, pp. 61–73, 2001.

[11] G. Gerstein and B. Mandelbrot, "Random walk models for the spike activity of a single neuron," *Biophys. J.*, vol. 4, pp. 41–68, 1964.

[12] S. Hendry, H. Schwark, E. Jones, and J. Yan, "Numbers and proportions of GABA-immunoreactive neurons in different areas of monkey cerebral cortex," *J. Neurosci.*, vol. 7, pp. 1503–19, 1987.

[13] P. König, A. K. Engel, and W. Singer, "Integrator or coincidence detector? The role of the cortical neuron revisited," *Trends in Neurosciences*, vol. 719, no. 4, pp. 130–137, 1996.

[14] A. Kuhn, A. Aertsen, and S. Rotter, "Higher-order statistics of input ensembles and the response of simple model neurons," *Neural Computat.*, vol. 15, no. 1, pp. 67–101, 2003.

[15] S. Mikula and E. Niebur, "The effects of input rate and synchrony on a coincidence detector: Analytical solution," *Neural Computat.*, vol. 5, no. 3, pp. 539–47, 2003.

[16] ——, "Synaptic depression leads to nonmonotonic frequency dependence in the coincidence detector," *Neural Computat.*, vol. 15, no. 10, pp. 2339–58, 2003.

[17] E. Niebur and C. Koch, "A model for the neuronal implementation of selective visual attention based on temporal correlation among neurons," *J. Computat. Neurosci.*, vol. 1, no. 1, pp. 141–158, 1994.

[18] E. Niebur, C. Koch, and C. Rosin, "An oscillation-based model for the neural basis of attention," *Vis. Res.*, vol. 33, pp. 2789–2802, 1993.

[19] G. F. Poggio and L. J. Viernstein, "Time series analysis of impulse sequences of thalamic somatic sensory neurons," *J. Neurophysiol.*, vol. 27, pp. 517–545, 1964.

[20] N. Qian and T. J. Sejnowski, "When is an inhibitory synapse effective?," *Proc. Nat. Acad. Sci. USA*, vol. 87, no. 20, pp. 8145–9, 1990.

[21] A. S. Ramoa, M. Shadlen, B. C. Skottun, and R. D. Freeman, "A comparison of inhibition in orientation and spatial frequency selectivity of cat visual cortex," *Nature*, vol. 321, no. 6067, pp. 237–239, 1986.

[22] L. M. Ricciardi, *Diffusion processes and related problems*. New York: Springer-Verlag, 1977.

[23] E. Salinas and T. J. Sejnowski, "Impact of correlated synaptic input on output firing rate and variability in simple neuronal models," *J. Neurosci.*, vol. 20, no. 16, pp. 6193–6209, 2000.

[24] ——, "Impact of correlated synaptic input on output firing rate and variability in simple neuronal models," *J. Neurosci.*, vol. 20, no. 16, pp. 6193–6209, 2000.

[25] M. N. Shadlen and W. T. Newsome, "Noise, neural codes and cortical organization," *Current Opinion Neurobiol.*, vol. 4, pp. 569–579, 1994.

[26] M. Shadlen and W. Newsome, "Noise, neural codes and cortical organization," *Current Opinion Neurobiol.*, vol. 4, pp. 569–579, 1994.

[27] W. Softky, "Sub-millisecond coincidence detection in active dendritic trees," *Neurosci.*, vol. 58, no. 1, pp. 13–41, 1994.

[28] W. Softky and C. Koch, "Cortical cells should fire regularly but do not," *Neural Computat.*, vol. 4, no. 5, pp. 643–646, 1992.

[29] W. Softky and C. Softky, "The highly irregular firing of cortical cells is inconsistent with temporal integration of random EPSPs," *J. Neurosci.*, vol. 13, no. 1, pp. 334–350, 1993.

[30] P. N. Steinmetz, A. Roy, P. Fitzgerald, S. S. Hsiao, K. O Johnson, and E. Niebur, "Attention modulates synchronized neuronal firing in primate somatosensory cortex," *Nature*, vol. 404, pp. 187–190, 2000.

[31] S. Stroeve and S. Gielen, "Correlation between uncoupled conductance-based integrate-and-fire neurons due to common and synchronous presynaptic firing," *Neural Computat.*, vol. 13, no. 9, pp. 2005–29, 2001.

[32] H. C. Tuckwell, *Stochastic Processes in the Neurosciences*. Philadelphia, PA: SIAM, 1989.

[33] G. Werner and V. B. Mountcastle, "The variability of central neural activity in a sensory system and its implications for the central reflection of sensory events," *J. Neurophysiol.*, vol. 26, pp. 958–977, 1963.

Shawn Mikula received the B.S. degrees in mathematics, physics, and biochemistry (all with honors) from the University of Texas at Austin, in 1998. He is currently working toward the Ph.D. degree in neuroscience at The Johns Hopkins University, Baltimore, MD.

His research interests include neural systems analysis of the large-scale functional and anatomical organization in human and nonhuman primate brains through the utilization of anatomical (immediate-early-gene and immunocytochemical mapping), functional (fMRI), analytical, and computational methodologies. He also maintains related interests in neuroinformatics, database development, datamining, and the visualization of high-dimensional datasets.

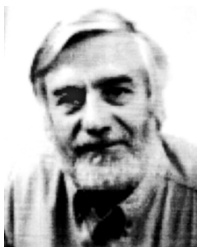

Ernst Niebur received the M.S. degree (Diplom-Physiker) from Universität Dortmund, Dortmund, Germany, in 1982 and the Ph.D. degree (Dr. és sciences) in physics from Université de Lausanne, Lausanne, Switzerland, in 1988. His Ph.D. dissertation topic was a computer simulation of the nervous system of the nematode *C. elegans*.

He was a Research Fellow and Senior Research Fellow at the California Institute of Technology, Pasadena, CA, and, in 1995, an Adjunct Professor at the Queensland University of Technology, Brisbane, Australia. He is now an Associate Professor of Neuroscience in the School of Medicine, The Johns Hopkins University, Baltimore, MD. His research interests are in Computational Neuroscience.

Dr. Niebur was awarded a Seymour Cray (Switzerland) Award in Scientic Computation in 1988, an Alfred P. Sloan Fellowship in 1997, and an NSF CAREER Award in 1998.